The Discrete Variational Conformal Technique for the Calculation of Strip Transmission-Line Parameters

RODOLFO E. DIAZ

Abstract—**This paper describes a new method of obtaining the transmission line properties of strip transmission lines whose geometrical configurations would make them difficult to analyze with other available techniques. The Discrete Variational Conformal (DVC) technique relies on conformal transformations to obtain the simplest possible representation of the Green function for the configuration of interest. This Green function is then used with an assumed charge distribution in the plane of the original configuration, and in a novel variational expression for the modal capacitance. The resulting equation is particularly well suited for numerical evaluation. Sample configurations are used to compare DVC to other techniques: Exact conformal mapping, Method of Moments, Full Wave solutions, and a Transverse Transmission Line Method. Two examples of application of DVC to asymmetric configurations are given.**

I. Introduction

THE CALCULATION OF the impedance and coupling parameters of strip transmission lines has been one of the most fertile areas of published research in microwave theory since the inception of the IEEE TRANSACTIONS ON MICROWAVE THEORY AND TECHNIQUES. The techniques available today to solve TEM or quasi-TEM problems can be broadly classified as belonging to one of the following classes:

1) exact, by direct conformal mapping, as in Cohn [1];

2) approximate, by conformal mapping, as in Cohn [2] or Shelton [3];

3) approximate, by solution of the total field, as in finite difference relaxation or network analogues;

4) approximate, by method of moments (MoM) with exact Green function, as in Kammler's approach [4];

5) approximate, by exact Green function with assumed charge distribution and variational capacitance expressions, as in Koul and Bhat's transverse transmission line method (TTLM) [5] or Das and Prasad [6];

6) approximate, by spectral domain or full wave method with exact Green function, as in Itoh and Mittra [7] or Davies and Mirshekar–Syahkal [8];

7) approximate, by finite elements;

8) approximate, by exact conformal transformations of the boundary with numerical solution of the field, as in Levy [9].

Manuscript received October 28, 1985; revised January 21, 1986.

The author is with Ford Aerospace and Communications Corporation, Aeronutronic Division, Newport Beach, CA 92658–9983.

IEEE Log Number 8607968.

The relative merits and drawbacks of most of these methods have already been pointed out in detail in the literature by several authors, and will not be discussed here. Instead, the justification for the new method lies in the general limitations of validity (or convenience) of the methods listed above. For instance, Kammler's method can be modified to include multiple dielectrics, but the price paid is an even slower computer run-time than in the homogeneous case. A viable alternative is to use the free-space Green function and to account for the dielectrics by solving for the polarization charges on their interfaces [10]; thus simplifying the problem, but increasing the computational load. On the other hand, Koul and Bhat's TTLM (which uses Crampagne's [11] Green function) and the Full Wave-Spectral Domain solutions, can handle multiple dielectrics readily, but they require boundary side-walls (see Fig. 1) to solve the problems. These side-walls and the requisite Fourier Sum form of the solution can be inconvenient in two ways:

First, most microwave circuit boards consist of many components printed on the same substrate, almost none of which are close to boundary walls. To approach this limit, the above mentioned methods must make the side-wall separation tend to a large value relative to the ground plane spacing, which in turn requires the Fourier sums to include more terms to achieve convergence. Second, when the strips are small compared to the side-wall separation, the Fourier sum will again require many more high-frequency terms to accurately represent the rise to infinity of the charge density at the edges of the strips.

The question of convenience and computer time can be illustrated by considering the solution for the structure of Fig. 2(a), the coupled trough-lines, or, even worse, Fig. 2(b); two structures in which the boundaries are not exclusively of the parallel plane type. Clearly, for MoM or Spectral Domain to analyze such a configuration would require treating the middle fin as another conductor. The asymmetric geometry of Fig. 2(b) rules out the possibility of simplifying the problem by calling the slot either an electric or a magnetic wall for the mode of interest.

In the body of the paper, DVC is first introduced by solving the configuration of Fig. 2(a) and outlining its extension to the problem of Fig. 2(b). The more practical case of Fig. 3 is then solved. This solution is then used to

0018-9480/86/0600-0714$01.00 ©1986 IEEE

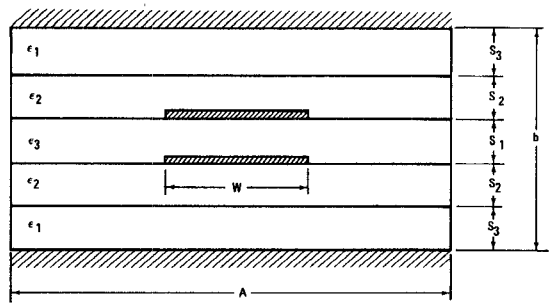

Fig. 1. Inhomogeneous stripline structure analyzable by full wave or spectral domain techniques with boundary side walls separated by the distance A.

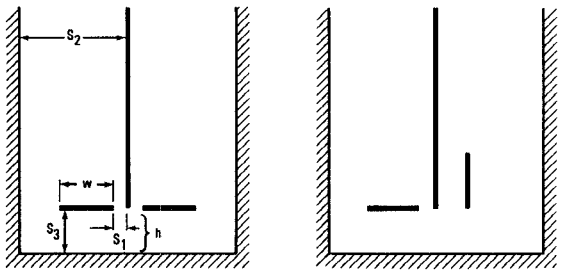

Fig. 2. Coupled trough lines: (a) Symmetric case. (b) Asymmetric case.

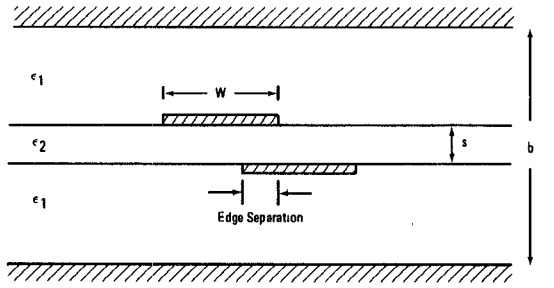

Fig. 3. Offset-coupled striplines with inhomogeneous dielectric.

compare DVC to other methods by solving for special cases which are, theoretically, within the bounds of validity of the different techniques involved.

It is shown that DVC is a useful complement to presently available techniques in solving TEM or Quasi-TEM problems when the geometry is not simple, while the resulting computer program is small and fast enough to run on a personal computer.

II. The Slot-Coupled Trough Lines

The purpose of this exercise is to illustrate DVC with a moderately complicated geometry which, in appropriate limits, can be analyzed by other methods. Thus, it is seen that in the limits of slot-width equal to zero and to infinity, the configuration of Fig. 2(a) reduces to the odd-odd and the even-odd modes of a four-strip transmission line as analyzed by Koul and Bhat [5] and also solvable by Kammler's method. Since only the even mode of this structure is not covered by Koul and Bhat's TTLM equations (the odd mode has an electric wall in the plane of

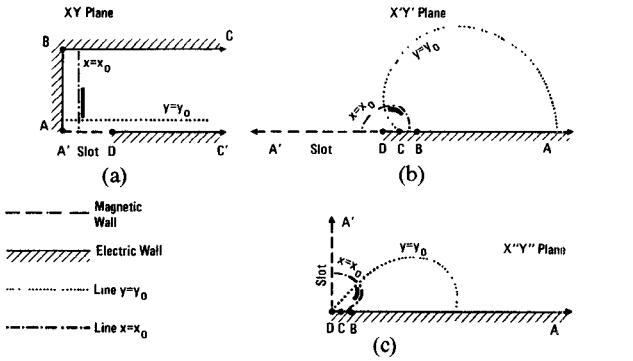

Fig. 4. Successive conformal transformations of the coupled trough lines of Fig. 2(a). (a) Original plane. (b) First map. (c) Second map. The successive deformations of the coordinate grid are illustrated by following the lines $x = x_o$, $y = y_o$.

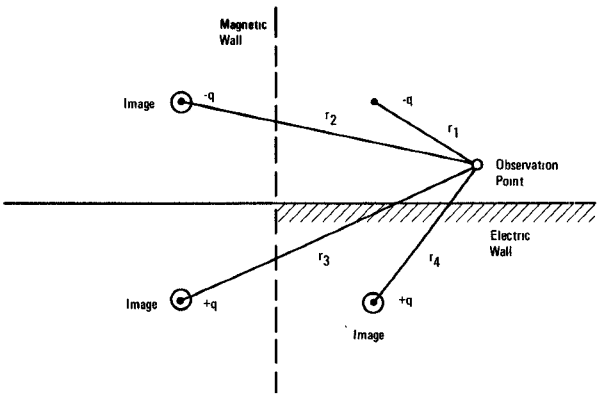

Fig. 5. The image charge system for a line charge in the presence of the boundary of Fig. 4(c).

symmetry thus reducing the slot-width to zero) only this mode needs to be solved for the purpose of this illustration.

The first step is to find the Green function. Fig. 4(a) shows the labeling of the vertices for the Schwarz–Christoffel mapping. Fig. 4(b) shows the result of this first transformation. To every charged point on the strip of Fig. 4(a), there is a corresponding charged point of equal strength in Fig. 4(b). If we were interested in the odd mode of the structure, we would stop at this point since then the line $A'D$ would be a zero potential and the Green function for a charged point above a flat ground plane is trivial. However, for the even mode another transformation is necessary to take Fig. 4(b) into Fig. 4(c). Again, all the charged points are merely redistributed in the new plane and the Green function for the even mode is elementary. For a charged point in the presence of the boundary of Fig. 5, the Green function is just

$$V = \frac{-q}{2\pi\epsilon} \ln\left(\frac{r_1 \cdot r_2}{r_3 \cdot r_4}\right). \tag{1}$$

Now, it is shown in the Appendix that the following expression for the capacitance is variational:

$$C = \int_x \frac{\rho(x)\,dx}{\int_{x'} \rho(x') V(x, x')\,dx'} \tag{2}$$

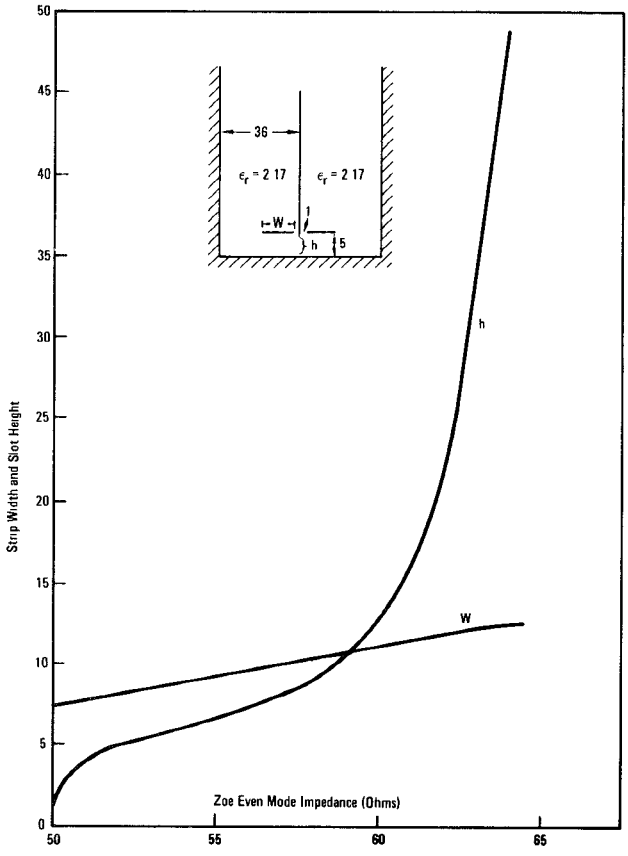

Fig. 6. Design curves for a pair of coupled trough lines.

where x, x' are points along the strip and $V(x, x')$ is the potential function normalized to a charge density of 1 coulomb/meter. This expression can be evaluated from its discrete analogue along the surface of the strip

$$C = \sum_n \frac{q_n}{V_n} \tag{3}$$

where q_n is the charge on the nth section of the strip and V_n is the potential on the nth section of the strip.

Because the potential function is transferred unaltered from one mapping to the next, as is the charge of a point, the computer program to perform this calculation merely has to perform the following steps.

1) Assume a charge distribution on the strip in the real configuration plane. A good charge distribution in most of these planar structures is just Maxwell's expression for the charge distribution on an isolated strip

$$\rho(x) = \frac{1}{\sqrt{1-\left(\dfrac{2(x-a/2)}{a}\right)^2}}, \qquad a = \text{Strip Width.} \tag{4}$$

2) Make this charge distribution discrete by evaluating it at N points and calling these points fixed charges.

3) Calculate from the conformal maps the connecting equations between positions in the real XY plane and the $X''Y''$ plane of Fig. 4(c) (this usually only involves elementary functions).

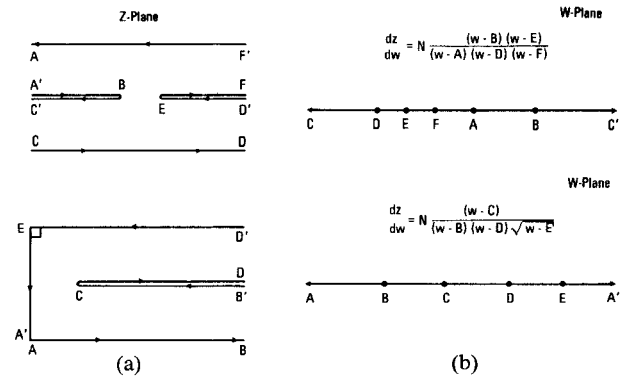

Fig. 7. Two possible ways of mapping the boundary of Fig. 2(b) onto a ground plane.

4) By summing over the strip in the $X''Y''$ plane, calculate the potential at a point adjacent to each of the N fixed charges.

5) Perform the sum of (3), where V_n and q_n are the potential and charge in each section of the strip.

Since the computer is only performing elementary function calculations and bookkeeping, the resulting program is extremely fast and inexpensive to run. The high speed of evaluation means that the analysis program can be used to synthesize a desired configuration by simple iteration. As an example, Fig. 6 is a plot of the strip width and slot width of the coupled lines of Fig. 2(a) as a function of *Zoe* (the even-mode impedance) for the matched system requirement that $\sqrt{Zoe*Zoo} = 50\ \Omega$ (the assumed system impedance).

To analyze the configuration of Fig. 2(b), a different conformal map is required. The bottom of the trough could be removed by using images, leaving a boundary that is easy to map (no right angles are involved) onto a flat ground plane. Alternatively, the bottom of the trough can be included by a map similar to the one used above, which has only one right angle. These two choices and their mapping derivatives are shown in Fig. 7. Now, two strips are involved instead of one but the computer algorithms are the same as before. The total potential is calculated at discrete points along the surface of each strip and (3) is used again. Clearly, the method does not require the strips to be of equal size although, as it was seen in the first example, it is easy to take advantage of any symmetries involved.

III. Offset-Coupled Lines with Arbitrary Center Dielectric

With the application of the exponential mapping to the configuration of Fig. 3, one can obtain Fig. 8. Thus, the Green function that we are looking for is that of a line charge in the presence of a dielectric wedge and a grounded plane. The motivation for going into the mapping plane to obtain the Green function is the following: When $\epsilon_2 = \epsilon_1$, the system reduces to the homogeneous case whose Green function is simple in the mapping plane (line charge above

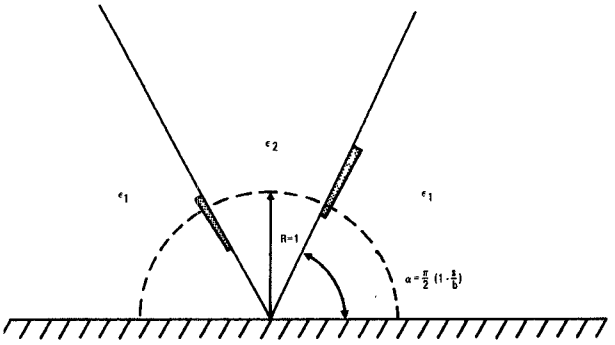

Fig. 8. Result of applying the exponential mapping to Fig. 3.

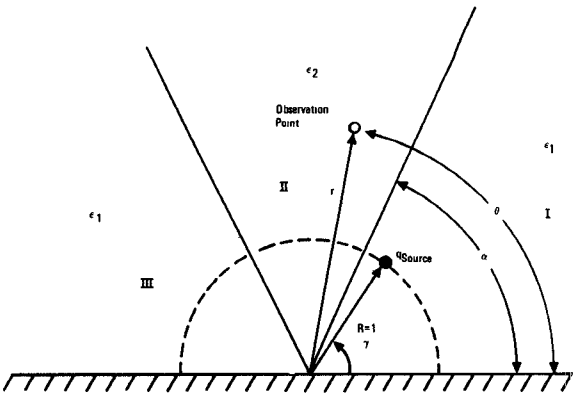

Fig. 9. Geometry used to find the Green function of Fig. 8.

ground) while it is rather complicated in the original plane (see Kammler [4]). Therefore, it is to be expected that the Green function for the inhomogeneous case will likewise be simpler. Once the problem is solved, this fact is proven.

Following the technique of Lewis and McKenna [12], the Boundary Value problem is solved via Mellin transforms. For reasons that will become clear later, we choose to place the charge at the point indicated in Fig. 9, and to let it approach the interface from the outer dielectric. All potentials are normalized to the unit charge in the outer dielectric so that in the homogeneous case, the potential due to a line charge above a ground plane would be

$$u = (1/2\pi) * \ln(r_1/r_2) \tag{5}$$

where r_1 and r_2 are the distances from the observation point to the charge and its image.

Lewis and McKenna [12] separate the problem into two parts. First, the homogeneous problem is solved. Then the solution to the inhomogeneous problem is expressed as the potential from the homogeneous part (the line charge) plus an added term (the dielectric polarization). Since the Mellin transform is given by

$$\bar{v}(\theta, s) = \int_0^\infty r^{s-1} v(r, \theta)\, dr \tag{6}$$

Poisson's equation for a delta function charge at $r=1$, $\theta = \gamma$, becomes

$$\bar{v}'' + s^2 \bar{v} = -\frac{1}{2\pi}\delta(\theta, \gamma) \tag{7}$$

which has a solution of the form ((7) of [12])

$$\bar{v}_1(\theta, s) = \begin{Bmatrix} \sin[s(\pi-\gamma)]\sin(s\theta)/[s\cdot\sin(s\pi)] \\ 0 < \theta < \gamma \\ \sin(s\gamma)\sin[s(\pi-\theta)]/[s\cdot\sin(s\pi)] \\ \gamma < \theta < \pi \end{Bmatrix}. \tag{8}$$

Then, the solution of the inhomogeneous problem in the three regions of Fig. 9 must be

$$\begin{aligned} &\text{I} \quad \bar{v} = \bar{v}_1 + B\sin(s\theta), \qquad 0 < \theta < \alpha \\ &\text{II} \quad \bar{v} = \bar{v}_1 + C\sin[s(\pi/2-\theta)] + D\cos[s(\pi/2-\theta)], \\ &\qquad\qquad\qquad\qquad\qquad\qquad \alpha < \theta < \pi - \alpha \\ &\text{III} \quad \bar{v} = \bar{v}_1 + E\sin[s(\pi-\theta)], \qquad \pi-\alpha < \theta < \pi. \end{aligned} \tag{9}$$

Matching boundary conditions at the two interfaces for the potential and the normal component of its derivative readily gives the expressions for the factors C and D as

$$\begin{aligned} C &= \frac{(1-\eta)\sin(s\alpha)\sin(s\gamma)\{\cos[s(\pi-\alpha)]+\cos(s\alpha)\}}{2s\sin(s\pi)\{\cos(s\alpha)\sin[s(\pi/2-\alpha)]+\eta\sin(s\alpha)\cos[s(\pi/2-\alpha)]\}} \\ D &= \frac{(1-\eta)\sin(s\alpha)\sin(s\gamma)\{\cos[s(\pi-\alpha)]-\cos(s\alpha)\}}{2s\sin(s\pi)\{\cos(s\alpha)\cos[s(\pi/2-\alpha)]-\eta\sin(s\alpha)\sin[s(\pi/2-\alpha)]\}} \end{aligned} \tag{10}$$

where $\eta = \epsilon_2/\epsilon_1$, and $\gamma \to \alpha$.

Since we are only interested in the potential on the interface, all we want is the solution in region II. This is accomplished by knowing C and D and applying the inverse transform. (If we are interested in calculating conductor losses, B and E can be obtained directly from C and D.) It is to be noted that the method of solution from here on differs from that of [12] in that the part of the solution due to the charge in the homogeneous medium is not absorbed into the potential of region II. Instead, we separate it explicitly, because its inverse Mellin transform is trivial (it must give the Green function of a line charge above a ground plane). This method of solution has the advantage of physical interpretation. Once the inverse Mellin transform is performed, we are left in region II with three terms: the first is the line charge term, or (5); the second is the symmetric part of the dielectric polarization; and the third is the antisymmetric part of the dielectric polarization. Thus, the contribution of the dielectric to the potential along the face on which the charge resides is just the sum of the second and third terms, while its contribution on the other face is the difference of these terms.

TABLE I
DEVELOPMENT OF THE EXPLICIT FORM OF (12)

The Zeros of the Denominators of Equations (10) are of Four Kinds

(a) for s = sdo = Odd

$$num_o = -2\cos(s\alpha)$$
$$den_o = \pi(-1)\,[\cos(s\alpha)\cos[s(\tfrac{\pi}{2}-\alpha)] - \eta\sin(s\alpha)\sin[s(\tfrac{\pi}{2}-\alpha)]]$$

(b) for s = sd = sdo + ζ_1

$$num_d = \cos[s(\pi-\alpha)] - \cos(s\alpha)$$
$$den_d = -\sin(s\pi)\,[\cos(s\alpha)\sin[s(\tfrac{\pi}{2}-\alpha)]\{\tfrac{\pi}{2}-\alpha(1-\eta)\} + \sin(s\alpha)\cos[s(\tfrac{\pi}{2}-\alpha)]\{\eta\tfrac{\pi}{2}+\alpha(1-\eta)\}]$$

(c) for s = sce = Even

$$num_e = +2\cos(s\alpha)$$
$$den_e = \pi(+1)\,[\cos(s\alpha)\sin[s(\tfrac{\pi}{2}-\alpha)] + \eta\sin(s\alpha)\cos[s(\tfrac{\pi}{2}-\alpha)]]$$

(d) for s = sc = sce + ζ_2

$$num_c = \cos[s(\pi-\alpha)] + \cos(s\alpha)$$
$$den_c = +\sin(s\pi)\,[\cos(s\alpha)\cos[s(\tfrac{\pi}{2}-\alpha)]\{\tfrac{\pi}{2}-\alpha(1-\eta)\} - \sin(s\alpha)\sin[s(\tfrac{\pi}{2}-\alpha)]\{\eta\tfrac{\pi}{2}+\alpha(1-\eta)\}]$$

Then, the Polarization Potential has a Symmetric Part Given by.

(e) $$\sum_{k=o,d} \frac{(1-\eta)\sin(s\alpha)\sin(s\gamma)}{2s}\,\frac{num_k}{den_k}\cos[s(\tfrac{\pi}{2}-\theta)]\,r^{-s}$$

and an Antisymmetric Part Given by.

(f) $$\sum_{k=e,c} \frac{(1-\eta)\sin(s\alpha)\sin(s\gamma)}{2s}\,\frac{num_k}{den_k}\sin[s(\tfrac{\pi}{2}-\theta)]\,r^{-s}$$

The inverse Mellin transform is given by

$$v(r,\theta) = \frac{1}{2\pi i}\int_{c-i\infty}^{c+i\infty} \bar{v}(\theta,s)\,r^{-s}\,ds \tag{11}$$

which is evaluated by the residue theorem. Thus, the potential due to the dielectric is given by

$$\sum_{\text{Res}} D\cos[s(\pi/2-\theta)]\,r^{-s} \pm \sum_{\text{Res}} C\sin[s(\pi/2-\theta)]\,r^{-s} \tag{12}$$

where the positive sign is taken for $\theta = \alpha$, the negative sign for $\theta = \pi - \alpha$. Using (10), the expression for the polarization potential is obtained. The results are summarized in Table I.

As Table I shows, all that needs to be done now is to find the zeros of (b) and (d) of Table I. Since the original motivation for solving this problem was to obtain design equations for the case $\epsilon_2 < \epsilon_1$ or $\eta < 1$, we chose to place the charge as shown in Fig. 9, in the outer dielectric. This allows the use of an efficient routine for finding the zeros of the equations as follows:

If η is close to 1.0, say $1.0-\delta$, then ζ_1 and ζ_2 in (b) and (d) of Table I are small.

By using the Taylor expansion of the trigonometric functions, it is easy to show that ζ_1 and ζ_2 are

$$\zeta_1 = \frac{2\delta}{\pi}\sin(sdo\cdot\alpha)\cos(sdo\cdot\alpha)$$
$$\zeta_2 = \frac{2\delta}{\pi}\sin(sce\cdot\alpha)\cos(sce\cdot\alpha). \tag{13}$$

Now successive approximations can be obtained by performing the following steps:

(a) Let

$$gnl = \frac{2\delta}{\pi}\,\frac{\sin(sd\cdot\alpha)\sin[sd(\pi/2-\alpha)] + \cos(sd\cdot\pi/2)}{\sin(sd\cdot\pi/2)}$$

(b) then $sd = sd + gnl$; return to (a)

(c) Let

$$fnl = \frac{2\delta}{\pi}\,\frac{\sin(sc\cdot\alpha)\cos[sc(\pi/2-\alpha)] - \sin(sc\cdot\pi/2)}{\cos(sc\cdot\pi/2)}$$

(d) then $sc = sc + fnl$; return to (c). (14)

Iterating 20 times is enough to guarantee the location of the zeros to better than 0.005 even in the extreme case of $\eta = 0.1$ (successive zeros are separated at least by 1.0). At this point it becomes clear why we chose to place the source charge outside the central wedge. This way, the quantity $(1-\eta)$ is always less than 1.0 and the search for the zeros converges readily. If we were interested in the suspended substrate case $\epsilon_2 > \epsilon_1$, $\eta > 1$, then it would be best to solve for the Green function with the charge inside the central wedge. When the zeros have been found, the problem is solved.

To implement the program, the polarization potentials are calculated for the geometry and the η desired. These are splined as potential-as-a-function-of-distance in the real configuration space. Then the same routine used for the trough lines is used; with the polarization potential being obtained from the spline and the line charge potential from the expression $(1/2\pi)*\ln(r_1/r_2)$ in the mapping plane. The impedances and effective dielectric constants are obtained from the classic equations

$$Z = \frac{1}{c\sqrt{C_o\cdot C_d}}$$
$$\epsilon_{\text{eff}} = \frac{C_d}{C_o} \tag{15}$$

where c is the speed of light, C_o is the capacitance in the absence of the dielectric, and C_d is the capacitance in the presence of the dielectric.

It is to be noted that for almost any configuration having striplines between parallel planes, Maxwell's distribution of charge is a good approximation. Intuition tells us that it would not be so for the configuration of Fig. 8; however, the conformal mapping has taken care of the situation. Since the positions of the discrete charges are picked at uniform intervals along the strips in the plane of Fig. 3, when the conformal transformation is applied, the points redistribute themselves on the new strips at nonuniform intervals to give a more realistic charge density distribution appropriate for Fig. 8.

There are at this point two sources of error. The first is the finite number of charged points chosen to describe the continuous charge distribution. The second is the fact that an approximate charge distribution has been chosen. The first will be addressed in the section below called Special Cases. The second is a compromise.

It is conceivable to pick different charge distributions to calculate the even-mode impedance, the odd-mode impedance, and the self impedance of the striplines in question. This would require three separate calculations. However, since the object of a variational approach is to obtain a

TABLE II
PERCENT DEVIATION OF THE VALUE AT CONVERGENCE FROM THE EXACT VALUE FOR TWO EXTREME CASES OF FIG. 10

	W = 0.10 S = 0.05	W = 1.0 S = 2.0
MoM	0.10%	0.28%
TTLM	4.50%	2.26%
DVC	1.36%	0.42%
DVC-S	0.79%	0.45%

good answer with a minimum of work, it is a reasonable expectation that one charge distribution be enough to calculate all impedances in question. This is what we have chosen to do, and the natural candidate for this all-purpose charge distribution is Maxwell's distribution for an isolated strip.

When a stripline component such as a symmetric coupler is to be designed, the geometry of the strips goes through a wide range of variations. To take full advantage of the one computer program in dealing with the whole design range, it is desirable to minimize the error introduced by the approximate charge distribution for that particular range. A method that works in practice is to modify the DVC self impedance of the isolated strip in the given stripline environment by a perturbation factor that will bring the DVC result as close as possible to the exact value of the self impedance of the isolated strip (as obtained by conformal mapping). One such factor is given in (16) and the effect of using this kind of self-impedance correction on the DVC results is seen in Table II by comparing the results labelled DVC with the corrected result labelled DVC-s.

$$f = 1 + 0.01 \cdot \left(1.363 \sqrt{\left(\frac{w}{b-s} \right)^2 + 0.54} - 1 \right). \quad (16)$$

In (16), the parameters are as illustrated in Fig. 3. This factor guarantees that the DVC self impedance of a strip symmetrically placed between ground planes ($s = 0$) will agree with the theoretical value, to better than 0.1 percent, up to $w/b = 4$.

To check the validity of the DVC solution, several special cases can be solved. The results are presented in the next section. Note that since the results only depend on relative dimensions, the units of length have been omitted. Most test cases were done assuming typical ground place spacings of 72 mils (1.829 mm) and a center substrate thickness of 10 mils (0.254 mm).

III. SPECIAL CASES

First, the case of Fig. 10 is solved. The symmetric homogeneous striplines have an exact conformal map solution.

Three computer programs will be compared on this problem. A program based on Kammler's MoM [13], a program based on Koul and Bhat's TTLM equations, and a DVC program. Two extreme cases of the configuration of Fig. 10 will be evaluated. The first is strips 0.1 units wide separated by 0.05 units, with a ground plane spacing of 1.0 units. The second is strips 1.0 units wide separated by 2.0 units, with a ground plane spacing of 1.0 units. The quantity to be computed is the system impedance or $\sqrt{Z_{even} \cdot Z_{odd}}$.

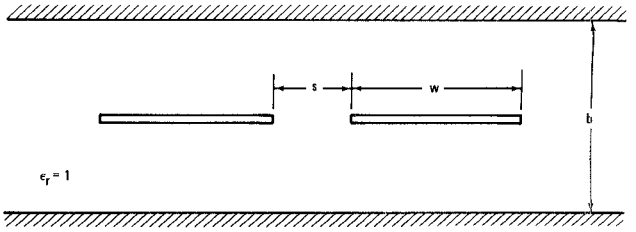

Fig. 10. The symmetric edge-coupled striplines.

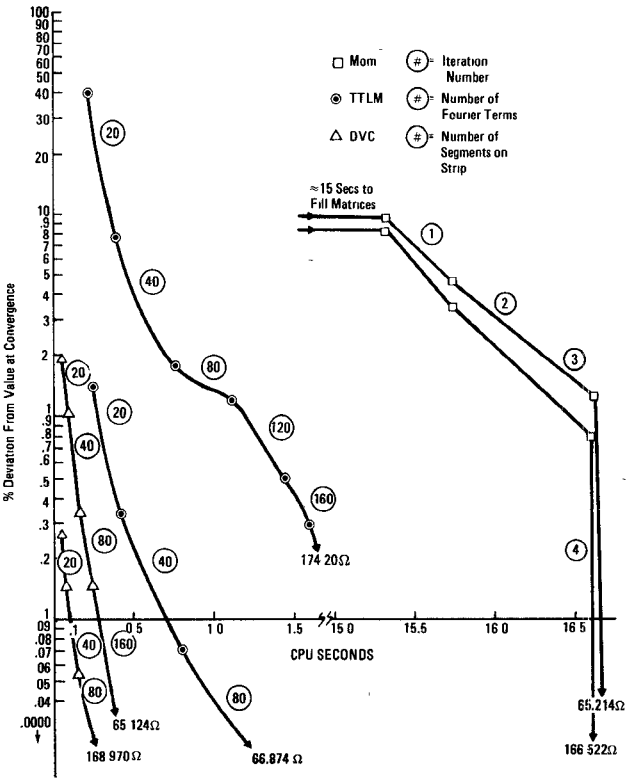

Fig. 11. The progression to convergence for two extreme cases of Fig. 10 for MoM TTLM and DVC. The values at convergence are shown.

Fig. 11 shows how each method approaches convergence as a function of CPU time spent. The ordinate of the graph shows the percent deviation from the final convergence value. Kammler's MoM iterates four times. First it cuts every strip in two parts, then in four, and finally in six, then it extrapolates to a final solution. The TTLM method achieves convergence by using an increasing number of Fourier components. The DVC method achieves convergence by dividing the strips into more parts.

Table II shows the percentage of error between the final value obtained at convergence and the exact conformal mapping value.

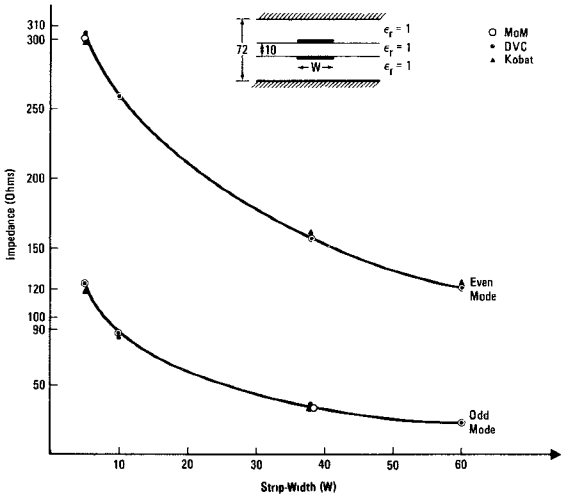

Fig. 12. Numerical solution of broadside-coupled striplines in a homogeneous medium.

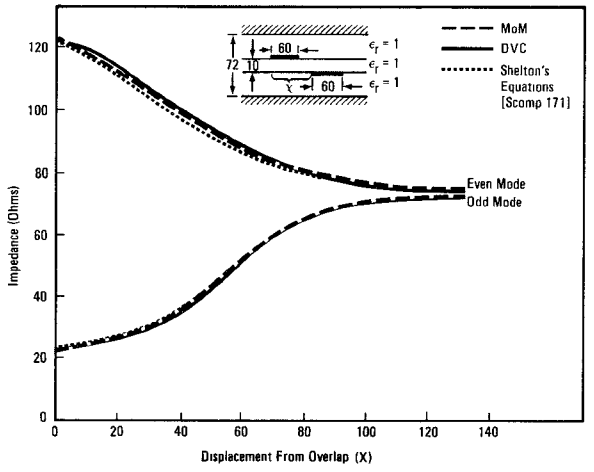

Fig. 13. Numerical solution of offset-coupled striplines in the wide strip limit.

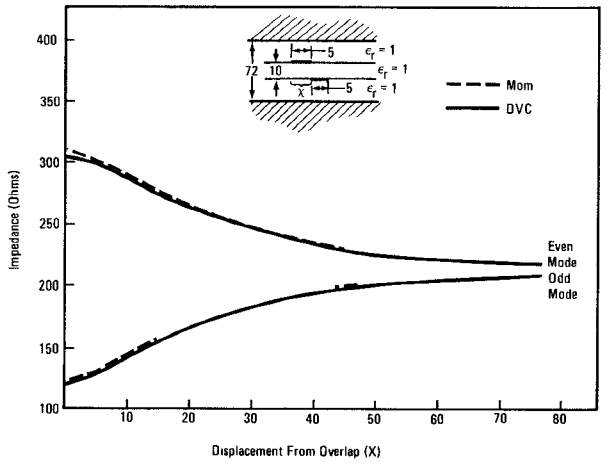

Fig. 14. Numerical solution of offset-coupled striplines in the small strip limit.

The practical requirement of less than 1-percent error for typical design configurations is easily met by the DVC method at the expense of very little CPU time.

The next test is to compare results for various techniques applied to broadside-coupled strips in the homogeneous

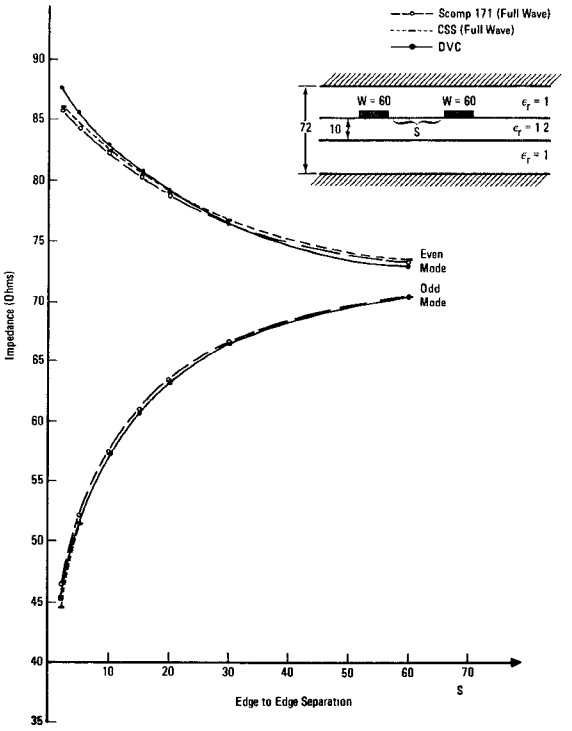

Fig. 15. Numerical solution of a suspended substrate configuration with substrate dielectric constant $\epsilon_r = 1.2$.

case. Fig. 12 is a comparison between MoM, TTLM, and DVC. The results are virtually identical.

Then, Shelton-offset-coupled lines in a homogeneous medium are checked. In the large strip limit, MoM, DVC, and Shelton's equations are compared in Fig. 13. In the small strip limit, MoM and DVC are compared in Fig. 14.

Finally, the suspended substrate for a center dielectric constant of 1.2 is checked using DVC, CSS [14], and the Coupled Suspended Substrate routines of Supercompact [15] for the case of wide strips (worst case for DVC). The results are given in Fig. 15. Over the range of specific cases tested, the DVC-based program performs as well or better than the other techniques.

IV. Two-Dielectric Shelton Offset-Coupled Lines

DuHammel Magic-T's are known to exhibit less than ideal isolation due to the difference in mode velocities when the lines are abruptly separated at the end of the T [16]. It has been proposed and empirically observed that by lowering the center dielectric constant in this region, these velocities can be equalized and the isolation improved. A feasible tradeoff is to print the whole circuit in a configuration with a lower center dielectric constant and to tolerate the slight dispersion along most of the line (which is low because the coupling is low) to achieve the benefit of equalized velocities at the discontinuity. Such a Magic-T has been designed and its experimental characteristics are described in a companion paper [17].

The design is achieved as follows. Starting from the broadside-coupled case, the strip widths are fractionally increased and the DVC program is iterated until an offset

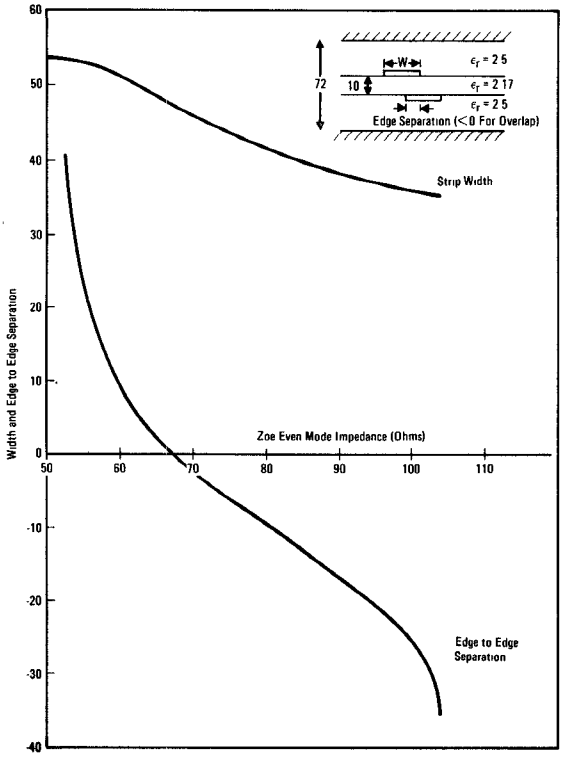

Fig. 16. Design curves for a possible two-dielectric offset-coupled stripline configuration.

is found which brings the system impedance back to 50 Ω. The widths are again increased and the cycle repeats, until the strips are decoupled. Because of the speed of program execution, the table of widths, offsets, and impedances can be made as precise as possible (the values only need to be better than the manufacturing tolerances) and the results then splined for use in the design program.

Fig. 16 is a plot of width and offset versus even-mode impedance of a possible geometry. When the strips are fully overlapped in this inhomogeneous case, the impedance as a function of a strip width can be compared to the calculations of Koul and Bhat [18] and those of Bahl and Bhartia [19]. The results are equivalent within the error bounds observed in Table II.

V. Conclusions

Certain boundary value problems with a low degree of symmetry, which arise in the design of strip transmission-line components are best solved by transforming the configuration in question to a new plane where the Green function is easier to evaluate. It is then straightforward to take advantage of the bookkeeping abilities of computing machines to calculate the desired parameters. In practice, an expression for charge on a strip equal to Maxwell's result for an isolated strip is used in the planar geometry. A typical strip is segmented into 80 parts and the charge is evaluated on the odd numbered sections, while the potential is evaluated on the even numbered sections. By using a new variational expression for the capacitance as a discrete sum of elementary capacitances, the results obtained from the computer program are fast and accurate to better than 1 percent in the design range of interest.

Appendix
The Capacitance Expression

Consider the following quantity, where $f(x, x')$ is the potential function with source at x and observer at x'

$$\Xi = \int_x \frac{\rho(x)\,dx}{\int_{x'} \rho(x') f(x, x')\,dx'}. \tag{A1}$$

Then define

$$\Xi_o = \int_x \frac{\rho_o(x)\,dx}{\int_{x'} \rho_o(x') f(x, x')\,dx'} \tag{A2}$$

with the property that

$$\int_{x'} \rho_o(x) f(x, x')\,dx' = V_o \text{ and } \int_{x'} \rho_o(x')\,dx' = Q_o \tag{A3}$$

where V_o is independent of x, and so that $\Xi_o = C_o$, the exact capacitance. Now let

$$\rho(x) \to \rho_o(x) + \delta\rho(x) \tag{A4}$$

so that by (A1)

$$\Xi + \delta\Xi = \int_x \frac{\rho_o(x)\,\delta\rho(x)}{\int_{x'} \rho_o(x') f(x, x')\,dx' + \int_{x'} \delta\rho(x') f(x, x')\,dx'}\,dx \tag{A5}$$

and by (A3)

$$\Xi + \delta\Xi = \frac{1}{V_o} \int_x \frac{\rho_o(x) + \delta\rho(x)}{1 + \int_{x'} \frac{\delta\rho(x') f(x, x')\,dx'}{V_o}}\,dx. \tag{A6}$$

Since the denominator is of the form $1+\epsilon$, $\epsilon \to 0$, expand in a Taylor series up to first order

$$\Xi + \delta\Xi = \frac{1}{V_o}\left\{ \int_x (\rho_o(x) + \delta\rho(x)) \cdot \left(1 - \int_{x'} \frac{\delta\rho(x') f(x, x')}{V_o}\,dx'\right) dx \right\} \tag{A7}$$

which becomes

$$\Xi + \delta\Xi = \frac{Q_o}{V_o} + \frac{\delta Q}{V_o} - \frac{1}{V_o} \int_x \rho_o(x) \int_{x'} \frac{\delta\rho(x') f(x, x')\,dx'\,dx}{V_o} - \frac{1}{V_o} \int_x \delta\rho(x) \int_{x'} \frac{\delta\rho(x') f(x, x')\,dx'\,dx}{V_o} \tag{A8}$$

where, by interchanging the order of integration we obtain

$$\Xi + \Delta\Xi = \frac{Q_o}{V_o} + \frac{\delta Q}{V_o} - \frac{1}{V_o} \int_{x'} \delta\rho(x') \frac{\int_x \rho_o(x) f(x, x')\,dx\,dx'}{V_o} - \frac{1}{V_o} \int_{x'} \int_x \frac{\delta\rho(x)\,\delta\rho(x') f(x, x')\,dx\,dx'}{V_o} \tag{A9}$$

and by (A2)

$$\Xi + \delta\Xi = \frac{Q_o}{V_o} + \frac{\delta Q}{V_o} - \frac{1}{V_o}\int_{x'} \delta\rho(x')\frac{V_o}{V_o}\,dx' - \frac{1}{V_o^2}\int_x\int_{x'} \delta\rho(x)\,\delta\rho(x')f(x,x')\,dx\,dx' \quad \text{(A10)}$$

or

$$\Xi + \delta\Xi = \frac{Q_o}{V_o} + \frac{\delta Q}{V_o} - \frac{\delta Q}{V_o} - \frac{1}{V_o^2} \qquad (\text{term of order } \delta\rho^2) \quad \text{(A11)}$$

thus

$$\Xi + \delta\Xi = \Xi_0 + 0(2) = C_0 + 0(2). \quad \text{(A12)}$$

That is, $\delta\Xi$ is 0(2).

Therefore, if Ξ is the capacitance, then a variation in $\rho(x)$, the charge density, gives only a second-order variation in Ξ. Ξ is variational and different from the usual

$$C = \frac{\left[\int \rho(x)\,dx\right]^2}{\int\int \rho(x)\rho(x')f(x,x')\,dx\,dx'}. \quad \text{(A13)}$$

Physically, Ξ corresponds to a parallel sum of elementary capacitances.

References

[1] S. B. Cohn, "Shielded coupled-strip transmission line," *IRE Trans. Microwave Theory Tech.*, vol. MTT-3, pp. 29–38, Oct. 1955.

[2] S.B. Cohn, "Characteristic impedances of broadside-coupled strip transmission lines," *IRE Trans. Microwave Theory Tech.*, vol. MTT-8, pp. 633–637, Nov. 1960.

[3] J.P. Shelton, "Impedances of offset parallel-coupled strip transmission lines," *IEEE Trans. Microwave Theory Tech.*, vol. MTT-14, pp. 7–15, Jan. 1966.

[4] D.W. Kammler, "Calculation of characteristic admittances and coupling coefficients for strip transmission lines," *IEEE Trans. Microwave Theory Tech.*, vol. MTT-16, pp. 925–937, Nov. 1968.

[5] S.K. Koul and B. Bhat, "Broadside, edge-coupled, symmetric strip transmission lines," *IEEE Trans. Microwave Theory Tech.*, vol. MTT-30, pp. 1874–1880, Nov. 1982.

[6] B. N. Das and K.V.S.V.R. Prasad, "A generalized formulation of electromagnetically-coupled striplines," *IEEE Trans. Microwave Theory Tech.*, vol. MTT-32, pp. 1427–1433, Nov. 1984.

[7] T. Itoh and R. Mittra, "A technique for computing dispersion characteristics of shielded microstrip lines," *IEEE Trans. Microwave Theory Tech.*, vol. MTT-22, pp. 896–898, Oct. 1974.

[8] J.B. Davies and D. Mirshekar-Syahkal, "Spectral domain solution of arbitrary transmission line with multilayer substrate," *IEEE Trans. Microwave Theory Tech.*, vol. MTT-25, pp. 143–146, Feb. 1977.

[9] R. Levy, "Conformal transformations combined with numerical techniques, with applications to coupled-bar problems," *IEEE Trans. Microwave Theory Tech.*, vol. MTT-28, pp. 369–375, Apr. 1980.

[10] S.M. Rao, T.K. Sarkar, and R.F. Harrington, "The electrostatic field of conducting bodies in multiple dielectric media," *IEEE Trans. Microwave Theory Tech.*, vol. MTT-32, pp. 1441–1448, Nov. 1984.

[11] R. Crampagne, M. Ahmadpanah, and J. L. Guiraud, "A simple method for determining the Green's function for a large class of MIC lines having multilayered dielectric structures," *IEEE Trans. Microwave Theory Tech.*, vol. MTT-26, pp. 82–87, Feb. 1978.

[12] J. A. Lewis and J. McKenna, "The field of a line charge near the tip of a dielectric wedge," *Bell Syst. Tech. J.*, vol. 55, no. 3, pp. 335–342, Mar. 1976.

[13] This program was written by Kammler for the Naval Weapons Center and it was provided to the author as a courtesy of J. Mosko of NWC.

[14] CSS is a version of the programs ZERO1 and ZERO2 by Davies and Mirshekar-Syahkal, due to Vaddiparty of Ford Aerospace's Western Development Laboratory, Palo Alto, CA.

[15] SuperCompact version 1.7, from Compact Software Inc., was used.

[16] C.P. Tresselt, "Design and computed theoretical performance of three classes of equal-ripple nonuniform line couplers," *IEEE Trans. Microwave Theory Tech.*, vol. MTT-17, pp. 218–230, Apr. 1969.

[17] R.E. Diaz and S. Seward, "Characteristics of the inhomogeneous stripline Magic-T," to be published.

[18] B. Bhat and S.K. Koul, "Unified approach to solve a class of strip and microstrip-like transmission lines," *IEEE Trans. Microwave Theory Tech.*, vol. MTT-30, pp. 679–686, May 1982.

[19] I.J. Bahl and P. Bhartia, "Characteristics of inhomogeneous broadside-coupled striplines," *IEEE Trans. Microwave Theory Tech.*, vol. MTT-28, pp. 529–535, June 1980.

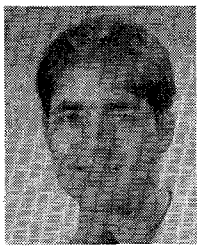

Rodolfo E. Diaz was born in Santurce, Puerto Rico, on June 17, 1958. He received the B.S. degree in physics from Yale University in 1978, the M.S. degree in physics from UCLA in 1980. From 1981 through 1984, he was enrolled in the Electrical Engineering Department at UCLA, where he completed all course requirements and examinations for the Ph.D. program in Electromagnetics.

From 1978 to 1983, he was a member of the Electromagnetic Effects Group at Rockwell International's Space Division. He joined the Radar Engineering Activity at Ford Aerospace, Aeronutronic Division, in 1983, where he has been working on the theory and application of broad-band stripline components and spiral antennas for antiradiation technology.